Catalytic Alkene Dimerization

DOI: 10.1002/ange.201008086

A Bifunctional Mechanism for Ethene Dimerization: Catalysis by Rhodium Complexes on Zeolite HY in the Absence of Halides**

*Pedro Serna and B. C. Gates**

Complexes of numerous transition metals catalyze C–C bond formation, and an enormous industrial production of oligomers and polymers from alkenes is carried out with complexes of early transition metals such as Cr, Ti, and Zr, some of them supported.[1–4] Late transition metals such as Ni, Pd, or Rh also catalyze these reactions, typically relying on halides, which allow the metal to shuttle between oxidation states in the catalytic cycle.[5,6] Active alkene oligomerization catalysts have also been prepared from complexes of late transition metals by incorporation of ligands such as those with neutral multidentate nitrogen donor groups.[7]

The formation of C–C bonds by dimerization of small alkenes such as ethene can take place on supported catalysts including reduced cobalt oxides,[8] nickel oxides,[9] and ruthenium clusters[10] in the presence of H_2, provided that the ratio of the H_2 to alkene partial pressures is low—but only with poor selectivities to *n*-butenes, typically $<1\,\%$ (the dominant reaction is hydrogenation of the C=C bond).

Now we show that site-isolated rhodium complexes supported on dealuminated zeolite HY (DAY zeolite), prepared from $[Rh(C_2H_4)_2(acac)]$ (acac = $CH_3COCHCOCH_3$), catalyze the dimerization of ethene in the absence of halides, with high selectivities to *n*-butenes (ca. 75 %), even when high partial pressures of H_2 are employed ($H_2/C_2H_4 = 4$, molar). The selective performance of this catalyst for C–C bond formation in the absence of labile ligands such as halides is a new and unanticipated result.

Characterization of the catalyst in the working state by IR and extended X-ray absorption fine structure (EXAFS) spectroscopies (even during catalysis with flowing mixtures of $C_2H_4 + H_2$ at 303 K and 1 bar) coupled with H/D exchange reaction experiments demonstrated that the catalysis involves a cooperation between mononuclear rhodium complexes and Brønsted acid sites of the zeolite support. H_2 promotes the dimerization reaction, which is accompanied by a slower hydrogenation of the C=C bond, and we infer that the ethyl species expected to be intermediates in the hydrogenation reaction[11] are not involved in the formation of the C–C bonds. Thus, the mode of action of the new dimerization catalyst differs both from that pertaining to halide-containing rhodium complexes[12–17] and that pertaining to strongly Brønsted acidic solids.[18–24]

The observation that site-isolated rhodium complexes supported on zeolite HY, initially present as $[Rh(C_2H_4)_2]$ (Table 1), catalyze the dimerization of ethene in a once-through plug-flow reactor at 1 bar and 303 K (with or without H_2 in the feed—the reaction is faster with H_2) is contrasted with our observation that the isostructural rhodium complexes supported on highly dehydroxylated MgO (Table SI-1 in the Supporting Information) are 100 % selective for hydrogenation of the C=C bond in the presence of H_2 and inactive under our conditions when C_2H_4 is used in the absence of H_2 (Table 2). The behavior of the MgO-supported catalyst agrees with reports demonstrating that Rh^I species require the participation of ligands (e.g., halides) to catalyze the alkene oligomerization.[12–14] For example, $[Rh(C_2H_4)_2(acac)]$, the precursor used to synthesize our zeolite- and MgO-supported catalysts, can be transformed into an active alkene dimerization catalyst by treatment with HCl.[12]

Table 1: EXAFS data at the Rh K edge characterizing the sample prepared by reaction of $[Rh(C_2H_4)_2(acac)]$ with the surface of zeolite DAY in gases flowing at 303 K.[a]

Gas in contact with sample	Shell	N	R [Å]	$10^3 \times \Delta\sigma^2$ [Å^2]	ΔE_0 [eV]
helium	Rh–Rh	–[b]	–[b]	–[b]	–[b]
	Rh–O	2.1	2.15	3.1	7.1
	Rh–C	3.7	2.08	3.4	−2.0
	Rh–Al	1.1	3.02	6.7	−2.5
$C_2H_4 + H_2$ (1:4)[c]	Rh–Rh	–	–	–	–
	Rh–O	2.0	2.13	2.4	2.6
	Rh–C	2.1	2.03	2.5	2.8
	Rh–Al	0.7	3.09	2.4	3.8
	Rh–C_{long}	1.8	3.05	1.8	9.2

[a] Notation: N, coordination number; R, distance between absorber and backscatterer atoms; $\Delta\sigma^2$, Debye–Waller factor; ΔE_0, inner potential correction. Error bounds (accuracies) characterizing the structural parameters obtained by EXAFS spectroscopy are estimated to be as follows: coordination number N, ±20%; distance R, ±0.02 Å; Debye–Waller factor $\Delta\sigma^2$, ±20%; and inner potential correction ΔE_0, ±20%. [b] Contribution not detectable. Details of the EXAFS fitting are provided in the Supporting Information. [c] Molar ratio.

---

[*] Dr. P. Serna, Prof. B. C. Gates
Department of Chemical Engineering and Materials Science
University of California
One Shields Avenue, Davis, CA 95616 (USA)
Fax: (+1) 530-752-1031
E-mail: bcgates@ucdavis.edu
Homepage: http://www.chms.ucdavis.edu/research/web/catalysis

[**] We acknowledge DOE Basic Energy Sciences for support (Contract No. FG02-04ER15513) and acknowledge beam time and support of the DOE Division of Materials Sciences for its role in the operation and development of beam line MR-CAT at the Advanced Photon Source at Argonne National Laboratory.

Supporting information for this article is available on the WWW under http://dx.doi.org/10.1002/anie.201008086.

Table 2: Catalytic results characterizing DAY zeolite-supported rhodium species for conversion of ethene at 303 K and 1 bar.

Predominant form of rhodium in catalyst[a]	TOF[b] $[s^{-1}]$	Product selectivity, molar ratio of dimers/ethane[e]
none[c]	–	–
$[Rh(C_2H_4)_2]$ [c]	0.075	3.55
$[Rh(C_2H_4)_2]$	0.012[d]	8.83
$[Rh(C_2H_4)_2]$	0.26[e]	2.63
Rh clusters (2–4 atoms each, on average)	0.93[f]	0.12
$[Rh(C_2H_4)_2]$[g]	0.025	0

[a] As determined by EXAFS and IR spectroscopies (details provided in the Supporting Information). [b] Turnover frequencies determined at time $t=0$ from the corresponding TOF vs. time-on-stream curves (see Supporting Information). [c] Reaction performed at 0.4 mbar of C_2H_4, 0.1 mbar of H_2, and 0.5 mbar of helium. [d] Reaction performed in the absence of H_2. [e] Reaction performed at 0.1 mbar of C_2H_4, 0.4 mbar of H_2, and 0.5 mbar of helium. [f] Constant once the composition of the feed had stabilized, approximately 5 min after the start of reactant flow. [g] Rhodium complexes supported on MgO.

The potential role of the zeolite itself as the catalyst for the C–C bond formation reaction is ruled out because its activity was too low to measure at 303 K (Table 2), as expected.[25,26] In the flow reactor containing the DAY zeolite without rhodium, $C_2H_4+H_2$ were observed to form traces of dimers (together with C_1, C_2, and C_3 hydrocarbons), but only at temperatures >433 K.

IR spectra show that the alkene interacted, on the one hand, with the zeolite through the acidic Al-OH groups, as indicated by the reduction in intensity of the O–H stretching bands at 3630 and 3565 cm^{-1} (Figure 1, top), which became strongly broadened and shifted to lower frequencies (Figure SI-1)[18,19] and, on the other hand, with the rhodium sites as well, as indicated by the disappearance of the bands at 3084, 3060, and 3016 cm^{-1} characterizing the C–H stretching vibrations in the ethene initially π-bonded to the Rh atoms (Figure 1, bottom).[27]

The C_2H_4–zeolite interaction is inferred to be weak, in agreement with the results of previous investigations,[25,28] as the C=C bond was retained upon ethene adsorption, as indicated by the appearance of an IR band at 1615 cm^{-1} (Figure SI-2), assigned to the C=C stretching vibration of ethene π-bonded to the acidic sites of the zeolite.[29] This result is consistent with the observation that the alkene readily desorbed from the acidic sites when helium flowed over the sample at room temperature, with full recovery of the initial Al–OH bands at 3630 and 3565 cm^{-1} (Figure SI-1).

On the other hand, the adsorption of ethene on the site-isolated rhodium species led to an almost instantaneous formation of alkyl species on the rhodium, indicated by the disappearance of the initially π-bonded ethene ligands and the concomitant growth of bands at 2960, 2935, and 2875 cm^{-1} assigned to stretching vibrations of $-CH$, $-CH_2$, and $-CH_3$ groups, as shown in Figure 1, bottom (consistent with this interpretation, no such change was observed when ethene flowed over the zeolite without rhodium). In agreement with these results, EXAFS data characterizing the catalyst in the working state show that the initial Rh–C coordination number of nearly 4 (corresponding to two π-bonded ethene ligands per Rh) decreased to 2.1 ± 0.4 upon introduction of $C_2H_4+H_2$ (Table 1), accompanied by the appearance of a second Rh–C contribution at a greater absorber–backscatterer distance, consistent with the formation of ethyl or butyl ligands. Furthermore, the EXAFS data gave no evidence of Rh–Rh contributions and thus no evidence of rhodium clusters, indicating the stability of the mononuclear rhodium complexes.[30]

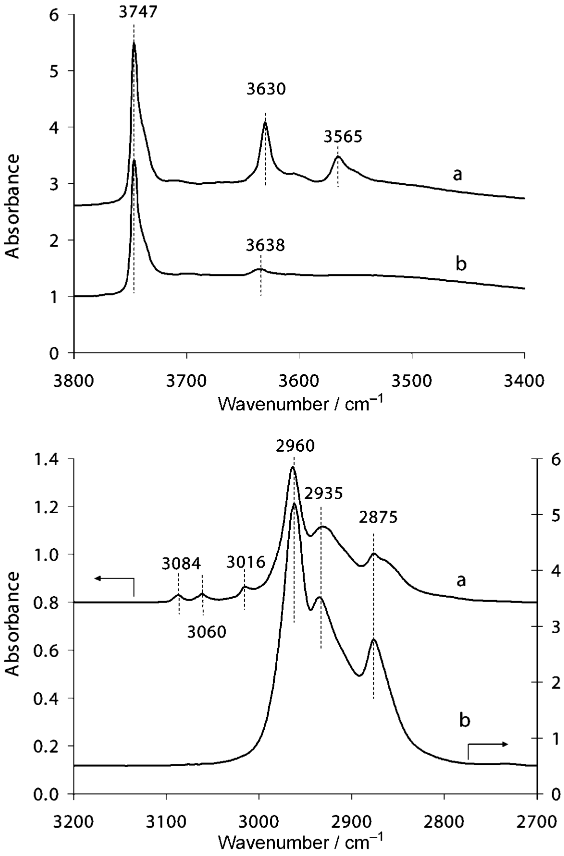

Figure 1. IR spectra in the $-OH$ (top) and $-CH$ (bottom) stretching regions characterizing the catalyst formed by reaction of $[Rh(C_2H_4)_2(acac)]$ with the surface of dealuminated HY zeolite after contact with a) flowing helium for 5 min and b) a reacting $C_2H_4+H_2$ mixture at 303 K and 1 bar. Spectrum (b) (bottom) was recorded with the sample in helium after removal of ethene from the gas phase by evacuation. Time-resolved IR spectra of the catalyst in the working state are shown in the Supporting Information.

The observation that neither rhodium complexes supported on MgO nor the DAY zeolite alone was catalytically active for ethene dimerization under our conditions (303 K, 1 bar), together with the spectroscopic data demonstrating the interactions of ethene with both the rhodium complexes and the acidic Al–OH groups of the support, indicates that both the rhodium and the Al–OH groups participate in the catalytic C–C bond-forming reaction.

To provide further understanding of the bifunctional reaction mechanism of the dimerization and the role of H_2, experiments were carried out with D_2 and with mixtures of D_2 and ethene. IR spectra of the zeolite-supported catalyst in flowing D_2 show that the −OH bands of the zeolite initially present at 3630 and 3565 cm^{-1} readily disappeared—as new bands grew in the range of 2550–2780 cm^{-1} (Figure SI-3), corresponding to the formation of Si−OD and Al−OD groups resulting from HD exchange.[29] Upon introduction of C_2H_4 to the IR cell, the Al−OD bands at 2677 and approximately 2600 cm^{-1} declined drastically in intensity (Figure SI-3)—just as the dimerization reaction started. Mass spectra of the gas-phase products show that the butenes were characterized by C_3H_5 and C_4H_8 fragments (*m*/*z* 41 and 56, respectively, corresponding to the typical fragmentation of *n*-butenes) with no deuterated dimers. This result demonstrates that C_2H_5 species, either as ethyl ligands formed on the rhodium after a partial hydrogenation of the initially π-bonded ethene ligands[31] or as carbenium ions on the acidic zeolite sites,[20] are not reaction intermediates in the formation of *n*-butenes, in contrast to the accepted mechanisms for dimerization of alkenes on halide-containing rhodium complexes[12,13] and on strong solid Brønsted acids.[18–24] (Scheme SI-1 illustrates the reported reaction mechanisms for ethene dimerization on these catalysts.) The results of the D_2 exchange experiments are thus consistent with the observation that ethene retained the C=C bond upon interaction with the zeolite Al−OH groups.

Moreover, the mass spectra characterizing the product observed with the zeolite-supported rhodium catalyst in the presence of flowing $C_2H_4 + D_2$ demonstrate the formation of C_2H_5D and $C_2H_4D_2$ in low concentrations, resulting from a minor, parallel hydrogenation of the C=C bond. Accordingly, we infer that this hydrogenation, in contrast to the dimerization process, proceeds through ethyl ligands on the rhodium, as expected.[31]

On the basis of these results, we propose a mechanism (Scheme 1) for the dimerization of ethene on the zeolite incorporating the rhodium complex. In this scheme, an ethene molecule weakly adsorbed on an Al−OH site of the zeolite (which is not reactive enough to couple with another ethene from the gas phase as occurs with stronger Brønsted acids) reacts with a second ethene molecule activated on a nearby rhodium site (Figure SI-7). According to this model, the two classes of active sites are required to be close enough to each other to allow a cooperative mechanism, consistent with our observation that a physical mixture of the bare H-form zeolite and the MgO-supported rhodium complex (5:1 mass ratio) led to the formation of ethane as the only observed reaction product, corresponding to the performance of the rhodium complex anchored to the basic support. Thus, we rule out the possibility that the dimerization occurs as a result of action of the acidic zeolite sites, even when hydrogen may spill over onto this support. However, we do not discard the possibility that the reaction takes place by activation of one of the ethene molecules on the same Al site where the rhodium complex is bonded, as it is known that the Al sites can be partially removed from the zeolite framework under some conditions to yield another type of acidic Al−OH species,[32] which we have observed for our catalyst in the presence of H_2 at 303 K and 1 bar, leading to the appearance of a new band in the −OH stretching region at 3710 cm^{-1} that readily disappeared upon contact with C_2H_4.

To account for the observed high selectivity to butenes (Table 2), we infer that the interaction between two adsorbed ethene molecules is faster than the hydrogenation of the C=C bond. The data indicate that the formation of the C−C bond, which is the rate-determining step when the reaction is catalyzed by rhodium halide complexes[12] and is quite slow on acidic zeolites,[20,21] is facilitated by a cooperation between the Rh^I species and the acidic sites of the support. In contrast, the accumulation of relatively large amounts of hydrocarbons on the surface of the catalyst during reaction (evidenced by intense IR bands in the range 2960–2875 cm^{-1}, Figure 1, bottom), together with the observed deactivation of the catalyst over time (Figure SI-6), suggests that product desorption might be rate-determining (notwithstanding the deactivation, more than 2000 turnovers of the catalyst were achieved in 5 h on stream, demonstrating that the reaction is catalytic). This observation, together with the fact that H_2 accelerates the dimerization reaction (Table 2) without being incorporated into the product butenes, suggests that the role of hydrogen is to facilitate the regeneration of the active sites by accelerating the desorption of the products.

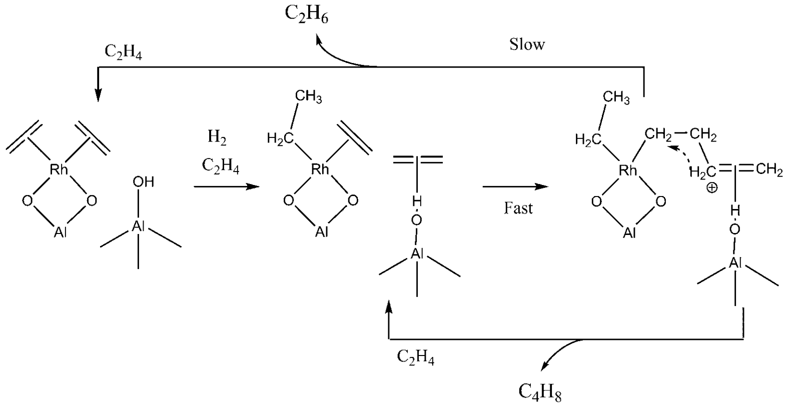

Scheme 1. Simplified reaction mechanism for the conversion of ethene on a zeolite-supported rhodium complex catalyst in the presence of H_2. The reaction intermediates are proposed on the basis of IR and EXAFS data, results of H_2/D_2 exchange experiments, and catalyst performance data.

To understand the role of the H_2 activation in the dimerization process, as well as in the competitive hydrogenation of the C=C bond, we compared the performance of the rhodium complex catalyst supported on zeolite DAY with that of a sample consisting of extremely small rhodium clusters on the same support, prepared by treatment of the former catalyst with H_2 at 303 K. EXAFS spectra taken at the Rh K edge after 1.2 h in flowing H_2 indicate a Rh−Rh coordination number of nearly 2 (Table SI-1), which corresponds to an average cluster nuclearity of 3, and thus to the presence of extremely small rhodium clusters together with unconverted rhodium complexes.[30]

The catalytic performance of the zeolite containing the rhodium clusters in flowing mixtures of $C_2H_4 + H_2$ at 303 K and 1 bar indicates that the hydrogenation of the double bond swamped the dimerization reaction kinetically—the overall reaction rate was more than three times that observed with the catalyst incorporating the site-isolated rhodium complexes, and the selectivity to ethane was high (Table 2). IR spectra characterizing the catalyst incorporating rhodium clusters in mixtures of $C_2H_4 + H_2$ demonstrate the appearance of a new band at 2091 cm^{-1} (Figure SI-4), assigned to a Rh–H species,[33] which was not observed for the supported mononuclear rhodium complexes. This comparison indicates that the activation of H_2 is faster on the rhodium clusters than on the rhodium complexes. Moreover, the IR data indicate that on the catalyst incorporating the rhodium clusters, ethene did not interact substantially with the acidic sites, as the initial Al–OH bands (at 3630 and 3565 cm^{-1}) remained unchanged upon introduction of the reactants (Figure SI-5). Thus, we infer that the equilibrium of the adsorption of C_2H_4 on the acidic sites of the zeolite incorporating the supported metal (i.e., $Al{-}OH + C_2H_4 \rightleftarrows Al{-}OH{-}C_2H_4$) was shifted to the left as the rate of the H_2 dissociation increased when rhodium clusters were present.

Thus, the activation of H_2 plays a key role in the catalytic behavior of the zeolite-supported rhodium species. On the catalyst containing the mononuclear rhodium complexes, H_2 is inferred to boost the dimerization reaction by facilitating the desorption of the products. Paradoxically, a too-fast activation of H_2, such as was observed when small rhodium clusters were present, largely impedes the activation of the ethene on the acidic sites of the zeolite (thereby inhibiting the dimerization according to the mechanism proposed in Scheme 1)—as demonstrated by the IR results—instead favoring the competitive hydrogenation on the rhodium sites. We emphasize, however, that the capability of the catalyst to produce butenes is not controlled merely by the H_2 dissociation rate, but is influenced by the presence of Rh/Al–OH pairs acting in concert, as the data show that rhodium complexes on MgO (which are relatively low in activity for hydrogenation (Table 2)) do not catalyze dimerization of the alkene under our conditions.

In summary, to our knowledge the results provide the first evidence of a cooperation between metal complexes and solid Brønsted acids in the formation of C–C bonds, demonstrating the activity of supported rhodium complexes for alkene dimerization in the absence of halides—with a high selectivity to *n*-butenes in an excess of H_2. The EXAFS and IR spectra and the results of the H/D exchange experiments indicate that the mode of action of the zeolite-supported rhodium complexes acting in concert with the adjacent acidic sites differs fundamentally from that pertaining to halide-containing rhodium complexes and strong Brønsted acids alone.

Received: December 21, 2010

Keywords: alkene dimerization · bifunctional catalysis · C–C bond formation · rhodium complexes · zeolites

[1] G. Natta, P. Pino, P. Corradini, F. Danusso, E. Mantica, G. Mazzanti, G. Moraglio, *J. Am. Chem. Soc.* **1955**, *77*, 1708.

[2] M. P. McDaniel, *Adv. Catal.* **1985**, *33*, 47; M. P. McDaniel, *Adv. Catal.* **2010**, *53*, 123.

[3] B. M. Weckhuysen, I. E. Wachs, R. A. Schoonheydt, *Chem. Rev.* **1996**, *96*, 3327.

[4] J. C. W. Chien, *Top. Catal.* **1999**, *7*, 23.

[5] *Metal-Catalyzed Cross-Coupling Reactions* (Eds.: F. Diederich, P. J. Stang), Wiley-VCH, Weinheim, **1998**.

[6] K. Fagnou, M. Lautens, *Chem. Rev.* **2003**, *103*, 169.

[7] S. Mecking, *Angew. Chem.* **2001**, *113*, 550; *Angew. Chem. Int. Ed.* **2001**, *40*, 534.

[8] R. J. Kokes, *J. Catal.* **1969**, *14*, 83.

[9] R. J. Kokes J. P. Bartek, *J. Catal.* **1979**, *12*, 72.

[10] E. Rodriguez, M. Leconte, J.-M. Basset, K. Tanaka, *J. Catal.* **1989**, *119*, 230.

[11] A. M. Argo, B. C. Gates, *J. Phys. Chem. B.* **2003**, *107*, 5519.

[12] R. J. Cramer, *J. Am. Chem. Soc.* **1965**, *87*, 4717.

[13] R. Cramer, *Inorg. Synth.* **1974**, *15*, 86.

[14] T. Alderson, E. L. Jenner, R. V. Lindsey, *J. Am. Chem. Soc.* **1965**, *87*, 5638.

[15] N. Takahashi, I. Okura, T. Keii, *J. Am. Chem. Soc.* **1975**, *97*, 7489.

[16] Y. Okamoto, N. Ishida, T. Imanaka, S. Teranishi, *J. Catal.* **1979**, *58*, 82.

[17] T. Yashima, Y. Ushida, M. Ebisawa, N. Hara, *J. Catal.* **1975**, *36*, 320.

[18] M. A. Makarova, V. L. Zholobenko, Kh. M. Al-Ghefaili, N. E. Thompson, J. Dewing, J. Dwyer, *J. Chem. Soc. Faraday Trans.* **1994**, *90*, 1047.

[19] V. B. Kazansky, I. R. Subbotina, F. C. Jentoft, *J. Catal.* **2006**, *240*, 66.

[20] S. Namuangruk, P. Pantu, J. Limtrakul, *ChemPhysChem* **2005**, *6*, 1333.

[21] S. Svelle, S. Kolboe, O. Swang, *J. Phys. Chem. B* **2004**, *108*, 2953.

[22] C. J. A. Mota, P. M. Esteves, M. B. de Amorim, *J. Phys. Chem.* **1996**, *100*, 12418.

[23] M. Boronat, P. Viruela, A. Corma, *J. Am. Chem. Soc.* **2004**, *126*, 3300.

[24] P. Viruela, A. Corma, *J. Phys. Chem. B* **2001**, *105*, 11169.

[25] E. G. Derouane, J.-P. Gilson, J. B. Nagy, *J. Mol. Catal.* **1981**, *10*, 331.

[26] N. W. Cant, W. K. Hall, *J. Catal.* **1972**, *25*, 161.

[27] A. J. Liang, V. A. Bhirud, J. O. Ehresmann, P. W. Kletnieks, J. F. Haw, B. C. Gates, *J. Phys. Chem. B* **2005**, *109*, 24236.

[28] B. V. Liengme, W. K. Hall, *Trans. Faraday Soc.* **1966**, *62*, 3229.

[29] J. N. Kondo, K. Domen, *J. Mol. Catal. A* **2003**, *199*, 27.

[30] A. J. Liang, B. C. Gates, *J. Phys. Chem. C* **2008**, *112*, 18039.

[31] Ref. [11].

[32] L. M. Parker, D. M. Bibby, G. R. Burns, *Zeolites* **1991**, *11*, 293.

[33] A. J. Liang, R. Craciun, M. Chen, T. G. Kelly, P. W. Kletnieks, J. F. Haw, D. A. Dixon, B. C. Gates, *J. Am. Chem. Soc.* **2009**, *131*, 8460.